Journal of Applied Fluid Mechanics, Vol. 12, No. 5, pp. 1487-1496, 2019.
Available online at www.jafmonline.net, ISSN 1735-3572, EISSN 1735-3645.
DOI: 10.29252/jafm.12.05.29674

Empirical and Numerical Analysis of Aerodynamic Drag on a Typical SUV Car Model at Different Locations of Vortex Generator

P. N. Selvaraju[1†] and K. M. Parammasivam[2]

[1]*Automobile Engineering, Rajalakshmi Engineering College, Chennai, Tamilnadu, 602105, India*
[2]*Aerospace Engineering, MIT Campus Anna University, Chennai, Tamilnadu, 600044, India*

†*Corresponding Author Email: selvarajumit@yahoo.co.in*

(Received September 28, 2018; accepted December 14, 2018)

ABSTRACT

The aerodynamic characteristics are concerned with the fuel consumption rate and the stability of a high speed vehicle. The current research aims at studying the aerodynamic behavior of a typical SUV vehicle model mounted with the vortex generator (VG) at various linear positions with reference to its rear roof edge. The flow field around the vehicle model was observed at different wind speed conditions. It had been determined that at the instance of lower wind speed, the VG had minimal effects of aerodynamic drag on the vehicle body. However, at the instance of higher wind speed conditions the magnitude of the drag force decreased significantly. Vehicles move at higher speeds in the highways, location of the VG varied towards the upstream of the vehicle due to early flow separation. Therefore test were conducted at different wind speeds and locations of VG. The numerical simulation conduced in this study provides flow characteristics around the vehicle model for different wind speeds. The realizable k−ε model was used to simulate and validate the empirical results in an effective manner. By using experimental data, the drag was reduced by 9.04 % at the optimized VG location. The results revealed that the induced aerodynamic drag would determine the best car shape. This paper provides a better understanding of VG positioning for enhanced flow separation control.

Keywords: Flow separation control; Vortex generator; VG location; Drag reduction; Boundary layer thickness.

NOMENCLATURE

A	projected frontal area
C_d	drag coefficient
C_P	pressure coefficient
D	drag force
L	length of car model
h	height of port
Re	Reynolds number
S	length of port
V	wind speed
θ	angle at port
ρ	density of air
υ	kinematic viscosity of air
δ	boundary layer thickness

1. INTRODUCTION

The flow of moving air relative to the car body has a direct effect on the stability, driving characteristics, operation, fuel consumption and the safety of car. The aerodynamic force plays an important role in the performance and the stability of the car when it takes high speed. Different types of aerodynamic forces such as drag, lift, and side forces are induced on car. The car experiences more drag when it takes high speed on the road.

Hence drag reduction is an essential process in vehicle aerodynamics for improving fuel consumption rate as well as the vehicle driving performance. Due to the increase in demand for automobiles that deliver a high performance along with safety and economy, there has been constant changes in the design of various parameters of an automobile, one such being the outer body and its shape. When car moves at higher speed, the aerodynamic drag force of vehicle is closely 80% of its total resistance. Fuel consumption increases by 50% since the aerodynamic drag is dominant at higher speed. The relationship between fuel

consumption and drag force coefficient is

$$\Delta FC/FC = \eta \times \Delta CD/CD \quad (1)$$

where FC - fuel consumption, CD - drag coefficient and η - the property of driving vehicle (0.5 to 0.7 for cars moving at higher speed). One of the suitable methods is the attachment of vortex generator externally on the car.

The objective of vortex generator (VG) is to reduce aerodynamic forces and to improve fuel efficiency of the car. Vortex generator's position from the tail edge of the car influences on the air flow patterns over a car body. Analysis of aerodynamic flow patterns acting on a vehicle and the resultant turbulences was carried out using computational fluid dynamics (CFD) and wind tunnel. The pressure difference between the front and rear end of car model, induced by the flow separation, leads to the pressure drag. To delay flow separation, delta shaped VG are tested at various positions of the roof of a scaled car model. The process involved scaled car modeling, analysis of aerodynamic flow over the car body, Comparison between the effect of aerodynamic flow patterns with and without VG.

Xu-xia Hu *et al* (2011) investigated the aerodynamic performance of high speed passenger car adopted with rear spoiler. A standard k − ε model was selected for the detailed study of numerical flow simulations. It was concluded that the aerodynamic drag got reduced by 1.7% and there was significant improvement in negative lift force of the car model. Harinaldi *et al*. (2011) analyzed aerodynamic drag on van model incorporated with suction and flowing on the rear side and delayed flow separation point. It had been observed that the aerodynamic drag reduction was 15.83% and 14.38% for suction and blowing air technique respectively. Li-Xin Guo *et al*. (2011) did comparison of the aerodynamic characteristics of two dimensional automobile shapes numerically. The results led to the conclusion that the vortex regions formed at the rear end of the automobile and air flow reverted again on the rear roof that induced drag. Till Heinemann *et al* (2012) investigated aerodynamic parameters of car model by using active flow control. Wind tunnel test was used to study flow field on profile over car model and laser Doppler anemometer was used to measure the velocity on the surrounding of the flow field. The results confirmed that wake induced at the below rear wind shield caused vortices and recirculation took further to car roof. Hitoshi Fukuda *et al* (1995) examined the aerodynamic characteristics car by measuring wake structure induced behind the car model mounted with rear spoiler. It had been shown that there was considerable reduction in lift and drag forces by both experimental and numerical results. Hasan Ali *et al* (2012) analyzed the drag reduction on car model by using VGs. The VGs were attached immediately upstream of the flow separation point in the rear edge of the car model. It was found that the VG' height was equal to the boundary layer thickness (15 to 25 mm) and delta shaped VGs were most suitable for effective reduction of aerodynamic drag force. Jahanmiri *et al* (2011) conducted experimental investigation of drag reduction on Ahmed car model by using combination of active flow control method. The suction of air at the flow separation point on the boundary layer and blowing air in the wake region were integrated. The results showed that the drag force reduced significantly compared with the existing method. Rakibul Hassan *et al* (2014) analyzed aerodynamic drag reduction on car model through a numerical process (Finite Volume Method) of solving the Favre-averaged Navier-Stokes equations backed by k – ε turbulence model. The rear under body modification and exhaust gas recirculation on the wake region were used to eliminate recirculation of air on rear roof and k-ε model was selected to study the air flow on the turbulent region. The results led to conclude that the drag could be decreased up to 22.13% by the modification of rear under body and up to 9.54% by the regulating of exhaust gas on the rear roof. Ram Bansal *et al* (2014) performed computations of drag reduction on passenger car using add-on devices. The aerodynamics of the most suitable design was studied by fixing vortex generator, spoiler, tail plates, and spoiler with VGs on flow separation point and evaluated the drag coefficient for passenger car. The results confirmed that the drag decreased significantly with the use of add-on devices. Xingjun *et al* (2011) investigated aerodynamic characteristics of sedan car model and the influence of different diffuser angles. The various parameters like diffuser, diffuser angle, the number of plates, the shape of separators, and the shape of the end plate were examined with respect to the under body flow and the wake. The total drag coefficients were greatly reduced at diffuser angle at 9.8°. Song *et al* (2012) investigated drag reduction by modifying rear shape of sedan car model. The aerodynamic variables optimized by changing rear body shape and flow field around the car profile were studied. The results revealed that the aerodynamic performance had improved by 5.64% when compared with the base model. Abdullah *et al* (2004) conducted an experimental investigation of flow around the sports utility vehicle. The aerodynamic parameters were studied experimentally and compared with the numerical results. It had been disclosed that more energetic vortex flow was induced in the centre plane of the model than that of its lateral plane position. Howell *et al* (2013) performed an empirical aerodynamic study on a typical reference model called Windsor body by implementing base pressure recovery technique for reducing the combined effects of drag and lift acting on the body. The crucial parameters viz., rear slant angle and rear taper length of the selected model were modified and its flow characteristics were recorded. The authors reported that the significant drag reduction was noticed at the instance of moderate rear taper angles, whereas there was a rapid rise in drag for a certain slant length of the model. Dirk Wieser *et al* (2014) conducted empirical and numerical studies of aerodynamic behavior of 1/4th reduced scale of

notchback and fastback car model called DrivAer. The surface pressure measurements were collected by varying the side wind configurations of the models considering the Reynolds number not greater than 3.2×10^6. The flow separation regions for both the models were observed post to the rear windshield zone. It had been observed that the notch back and fast back configurations exhibited the large asymmetrical and symmetrical flow pattern respectively downstream to the rear windshield region. Mahmoud Khaled et al (2012) dealt with experimental aerodynamic torsor characteristics of a simplified car model which was considered as a crucial parameter for regulating the under body flow configuration of the vehicle model. The authors came to the conclusion that the vertical air outlet technique would be the best optimal under body flow modifier among the other devices. The reduction of drag and pitch momentum coefficient for the particular configuration was calculated as 56.4% and 3.6% respectively relative to the base model. Hoonil Park et al (2013) did the experimental study of aerodynamic drag reduction on a simplified car geometry using synthetic jet array arrangement. The wind tunnel tests were performed on two configurations of an Ahmed body having 25° and 35° of rear slant angles with synthetic jet array positioned on the surface of the slant edge. The results revealed that the aerodynamic drag reduction was calculated as 5.2% relative to the base Ahmed model configured with 25° slant edge; however, the synthetic jet has increases in the drag characteristics of Ahmed model having 35° rear slant edge. Grosche *et al* (2001) conducted research on bluff body by controlling wake and air flow field. The flow patterns and trailing vortices parameters were examined in the dead water region of two different configurations like notchback and fastback models. The result were showed that the significant drag reduction could be obtained in the rear end modification and creating passive ventilation on under body. Jean Luc Aider *et al* (2010) investigated drag and lift forces on an Ahmed body with curved rear part. The location of VGs in longitudinal of curved shape and space between VGs were analyzed for better aerodynamic performance. The velocity field in the wake region and the interaction between VGs and over flow structure were examined using wind tunnel tests and PIV measurements. The results showed that maximum drag reduction of 12% and lift reduction of 60% were attained and further reduction achieved significantly through motorization of VG with respect to wind speed. Shubham Agarwal *et al* (2016) investigated the aerodynamic behavior on wing with the effect of VG location. The flow field measured on the wing with VG attached at various locations and angle attack varied. The results revealed that at small angles of attack of the wing, the VG had immaterial effects with a small decrease in lift and a small increase in drag. However, at larger angles of attack the lift increased and drag decreased significantly

In the literature surveyed, the drag reduction on vehicle by placing VG at a fixed position has been studied by Ram Bansal *et al* (2012), Jean Luc Aider *et al* (2010) and Hasan Ali *et al* (2012). The purpose of this study was to analyze drag reduction using VG. The current work studies the optimal positioning of VG, which reduces the drag on the vehicle, from the rear end for various wind speeds. Boundary layer thickness, flow separation point and pressure distribution at various points on the top surface of model were studied experimentally. Velocity contour, turbulent intensity gradient and pressure coefficient were studied numerically. The characteristics obtained experimentally were compared and analyzed numerically.

2. EXPERIMENTAL SET-UP

The aerodynamic drag and lift force acting on the testing model with respect to the appropriate wind speed were quantified by means of dual cantilever type load cell set-up connected with the two separate digital force indicators as shown in Fig. 2a. The sensitivity and data sampling rate of the aerodynamic drag and lift force measuring system was about 0.02N and 320 Hz respectively. The whole measuring set-up was kept under the raised floor system with a height of 0.1m from the bottom of the wind tunnel test section.

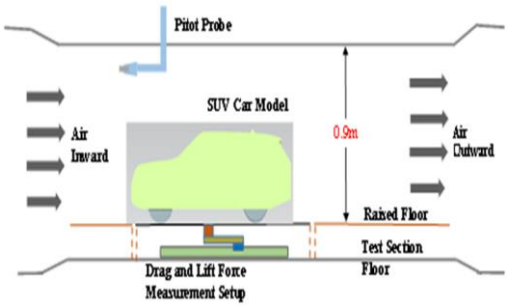

Fig. 2a. Experimental Set-Up.

The aerodynamic study of the 1/12th scaled car model was conducted using subsonic suction type wind tunnel. The subsonic wind tunnel facility could be viewed as an experimental facility. The wind flow was simulated in a controlled manner to represent the flow characteristics in the nature and the aerodynamic forces. The responses of the model were investigated in a scientific manner. The subsonic wind tunnel comprises Honey comb, contraction chamber, test section, and diffuser. The open circuit, suction type sub-sonic wind tunnel was utilized in this work and the same is shown in Fig. 2b. The test section of the wind tunnel has length 1.8 m, width 1.2 m and height 1 m and maximum wind speed of 30 m/s with propeller speed of about 150 rpm. The blockage ratio of wind tunnel is defined as the ratio of frontal area of the model to wind tunnel inlet test section area and it should not exceed 6 %. The blockage ratio for the chosen model was calculated as 2.2 % which is less than the permissible value hence the selected car model can be suitably tested in the wind tunnel section configuration.

Fig. 2b. Open type sub-sonic wind tunnel.

2.1. Car Model for Experimental Work.

The pressure tubes were connected to the port which was drilled around the car model as shown in Fig. 2c. The other ends of the tubes were connected with the ports available in the pressure scanner (64 bit). The pressure scanner was connected with the computer which displayed pressure values around the car model by using predetermined software. The measurement was carried out between wind speeds of 14.95 m/s and 27.01 m/s and the pressure values were tabulated.

Fig. 2c. Car model for experimental analysis.

3. EFFECT OF VORTEX GENERATOR ON AERODYNAMIC DRAG

A VG is an aerodynamic surface which has different shapes like rectangle, triangle and delta wing that tends to create a swirl in the fluid flow. Initially, VGs were widely used in the aerospace industry, mainly to control boundary layer transition and to delay flow separations. Different types of VG is used on race cars for manipulating the flow over and under the vehicle, mainly to generate down force and reduce drag force which is needed for better performance. Although the effect of such VGs was studied in the past, not all features of the flow fields were documented. The aerodynamic analysis was carried out using FLUENT software for different positions of VG on car model.

3.1. Design of Vortex Generators

A well-known type of VG shape is delta shape which has been analyzed by Gopal *et al* (2012). It has been tested by many researchers and found to give better aerodynamics performance on car model. The location of VG on car model and the dimensions of VG used for this work are shown in Fig. 3a-b. The purpose of using VG is to control flow separation at the roof of a car model; it is similar to the purpose of using VG on aircraft. To determine the shape and location of VGs, the data on aircraft VGs are referred.

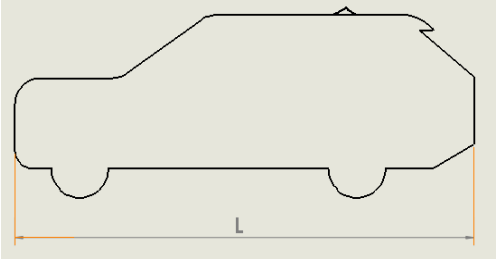

Fig. 3a. Car model with VG.

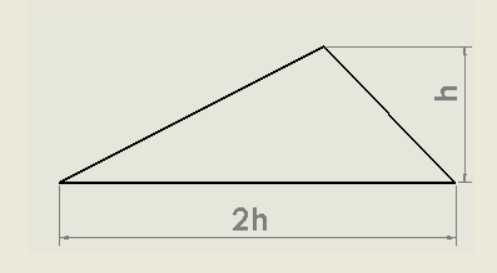

Fig. 3b. Delta shape vortex generator.

3.2. Calculation of Boundary Layer Thickness (δ)

From the Table 1, the height of the vortex generator (h) is taken as 9 mm approximately for the selected car model which is equal to boundary layer thickness as observed by Md. Hasan Ali *et al* (2012). The length and the thickness of the VG were calculated based on the height of VG.

Table 1 Calculation of boundary layer thickness

Parameters used	Values
Maximum wind speed (V)	27.01 m/s
Length of car model (L)	0.37 m
Kinematic viscosity of the air (υ)	18.4 m^2/s
Density of air (ρ)	1.296 kg/m^3
Reynolds number (Re)	5.43 x 10^5
Boundary layer thickness (δ)	8.9 mm

3.3. Calculation of Drag Force:

Drag coefficient $C_d = \int_0^{\pi} C_p \cos\theta \, \frac{s}{h}$ (2)

Where C_p=Pressure Coefficient, s = Length port, h= Height of the port, θ = Angle at port

Drag force $D = \frac{1}{2} C_d \, \rho A V^2$ (3)

Where V is the wind speed (m/s), A is the projected frontal area of the vehicle and ρ is the density of the ambient air.

Delta shaped VG is located on the roof of the car

at different position from the rear end at 40 mm, 50 mm, 60 mm, 70 mm and 80 mm. For each of the position of VG, experiments were conducted at each of the wind speeds 14.95 m/s, 17.03 m/s, 20.71 m/s, 22.88 m/s, 24.81 m/s and 27.01 m/s and the corresponding drag force was studied.

4. NUMERICAL SIMULATION

The CAD geometry of the scaled down car model was generated using modeling software for the entire computational study involved in this work. The tetrahedral mesh was used considering the setup time, computational time and numerical diffusion. The realizable k-ε model was used to analyze turbulent and wake region around the car model. The turbulent kinetic energy and the turbulent dissipation were visible by the second order upwind discretization method. The boundary condition used for numerical analysis is shown in Table 2. The maximum inlet air velocity was given as 27.01 m/s and based on the experiment conducted on the car model.

Table 2 Boundary condition for CFD analysis

Region	Boundary condition
Inlet	Velocity, V_{Min}=14.95 m/s & V_{Max}=27.01 m/s
Outlet	Pressure outlet, Reference pressure = 0 Pa
Top & Side	Wall & No slip
Ground	Wall & No slip
Turbulent model	Realizable k- ε model
Wall Y+ value	42

4.1. Computational Domain Dimension

The computational domain was generated by the modeling software and it covered the car geometry with its overall dimensional contingent being 10L, 4L, and 3L corresponding to the longitudinal axis, lateral axis, and vertical axis respectively of the car and prepared on the basis of the length of the car model (L).

The upstream and the downstream distances of fluid domain from the car model were designed 2L and 6L respectively. No slip boundary condition was applied to all the surfaces of the computational domain and the wall boundaries of the car model. To attain uniform flow in the inlet zone, boundary layer thickness was considered as zero and turbulence intensity value was given as 1%. Computational domain configuration with car model is shown in Fig. 4a. In addition to that Physics of the numerical flows was kept closer to the atmosphere of the experimental analysis. The inflation feature was utilized with the growth rate of 1.5 from the surface of the boundary. The inflation layers near the wall, VG and the rest of the fluid domain were meshed with tetrahedral elements as shown in Fig.4b. The non dimensional distance from the wall to the first layer which is referred as Y+ and the value calculated as 42 to reduce the number of element and computational time. The grid independence test was executed as shown in Table 3 earlier to the computational simulation since the number of cells in the fluid domain has significant impact on the CFD results.

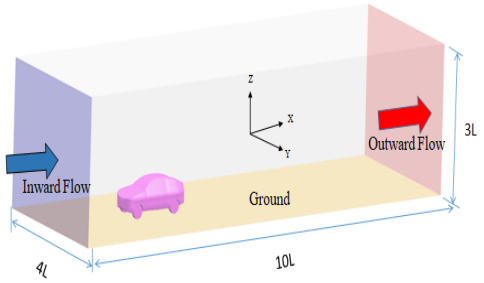

Fig. 4a. Computational domain with car model.

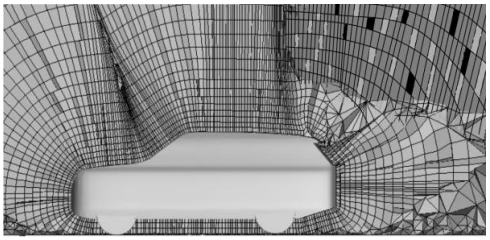

Fig. 4b. Mesh distribution at mid plane of the car model.

5. RESULT AND DISCUSSION

5.1. Pressure Coefficient on Base Model

The pressure coefficient was measured experimentally between the wind speeds 14.95 m/s to 27.01 m/s. Figure 5a shows the variation of pressure coefficient over profile of the car model with respect to different wind speeds. It is observed that high pressure is induced in the front part of the model, whereas low pressure is generated in the rear end of the model at all wind speeds. As the wind speed increases, the pressure drag on the car increases proportionately by Gopal *et al* (2012). At the rear part, the flow is detached due to adverse pressure gradient that causes pressure drag. It is evident that flow separation occurs at various positions from downstream to upstream of the fluid flow up to wind speed of 24.81m/s. The flow separation point was the same as of 24.81m/s even when the wind speed reached 27.01m/s due to fluid flow attachment at x/L of 0.6.

5.2. Location of Flow Separation Point from the Rear Edge with Wind Speed

From Fig. 5b, it is observed that the flow separation point changes with wind speed. Whenever the wind

Table 3 Grid independence test result

Total number of elements 1×10^6	First wall distance (mm)	Grid spacing ratio	Coefficient of drag	Time duration in (Hrs)
3.1	1.6	2.8	0.356	6
3.4	1.4	2.2	0.348	7
3.7	1.0	1.5	0.342	8
4.1	0.6	1.0	0.341	10

speed increases from 14.95 m/s to 17.03 m/s, the shift in flow separation point takes at 40 mm and 50mm approximately from the tail edge. When the wind speed changes from 20.71 m/s to 22.88 m/s, flow separation point moves at 60 and 70 mm from the tail edge. When the wind speed increases at 24.81 m/s, the flow separation point is dislocated at 80 mm. At this point, boundary layer suddenly thickens and causes adverse pressure gradient. The shear stress at this region is zero and it causes flow detachment. The fluid flow takes reverse direction due to detachment of the flow at this region and creates turbulent. When the wind speed is increased to 27.01 m/s, the flow separation point remains the same as of 24.8 m/s due to flow attachment on the boundary layer.

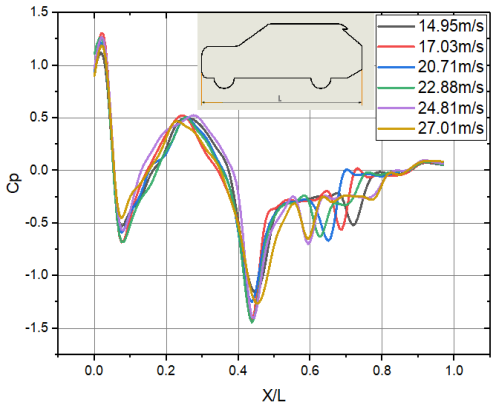

Fig. 5a. Variation of pressure coefficient with characteristics length.

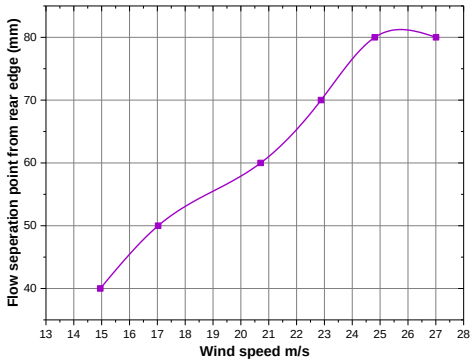

Fig. 5b. Variation of flow separation point with wind speed.

5.3. Pressure Distribution around the Car Model without and with VG

The figures 5c-h represents the pressure distribution around the car model is the same as before the fluid flow separation experimentally. The flow separation point varies from 40 mm, 50 mm, 60 mm, 70 mm, and 80 mm with respect to wind speeds. It is observed that the fluid flow takes separation from the fluid stream direction at x/L of 0.6-0.7 due to sudden change of pressure gradient. The single delta shape VG was used at flow separation point with respect to wind speeds in the mid section of car geometry. At the point of flow separation, the pressure curve is a straight line due to the presence of vortex generator located, whereas in the base model flow separation indicated by the line depression.

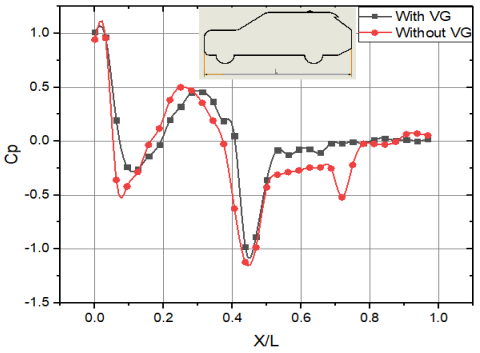

Fig. 5c. Variation of pressure coefficient at wind speed of 14.95 m/s.

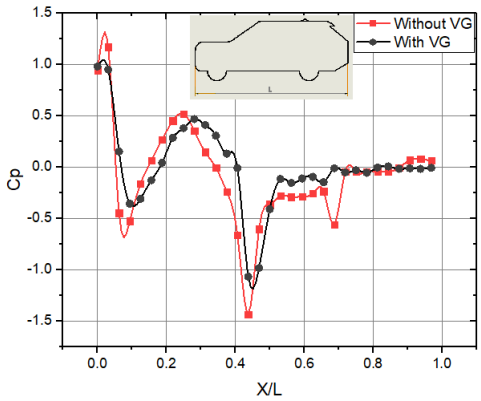

Fig. 5d. Variation of pressure coefficient at wind speed of 17.03 m/s.

6. DRAG FORCE

6.1. Effect of Wind Speed on Drag Force of the Base Car Model

Figure 6a shows variation of drag force with wind speed. It is clear that the drag is directly proportional to the wind speed. The experimental results led to the

conclusion that at higher wind speed, maximum drag forced was induced on car model.

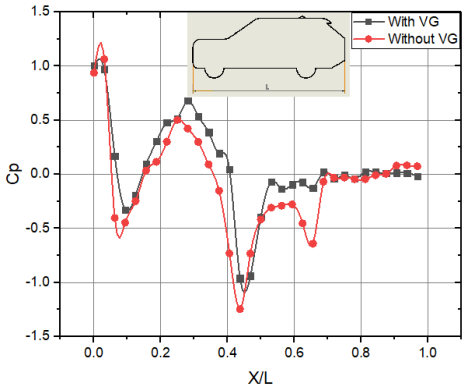

Fig. 5e. Variation of pressure coefficient at wind speed of 20.71 m/s.

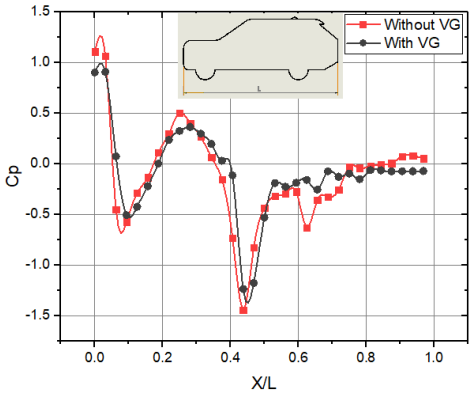

Fig. 5f. Variation of pressure coefficient at wind speed of 22.88 m/s.

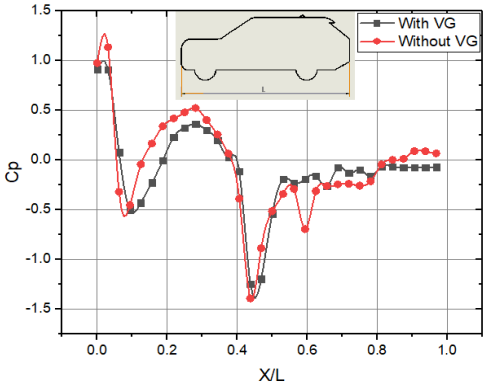

Fig. 5g. Variation of pressure coefficient at wind speed of 24.81 m/s.

6.2. Effect of VG location on Drag force

From the Fig. 6b, It is seen that the drag force decreases when the VG moves from the rear edge at all the wind speeds. When the VG is positioned at flow separation point from the rear edge, minimum drag force is induced on the car model. Hasan Ali *et al* (2012). The drag force increases continuously when the VG moves beyond flow separation point. Therefore, it is concluded that the location of the VG is optimized between 40 and 80 mm from the rear edge at wind speeds between 14.95 and 27.01 m/s for better drag reduction. When the wind speed is increased further, the flow separation point is maintained at the same point since the fluid flow thickens on the boundary of the car model.

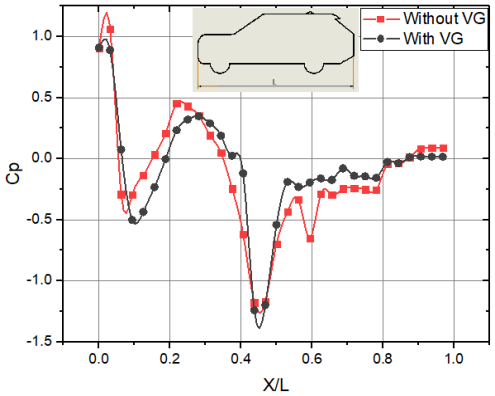

Fig. 5h. Variation of pressure coefficient at wind speed of 27.01 m/s.

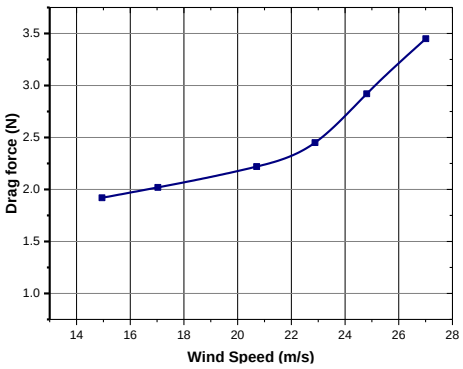

Fig. 6a.Variation of drag with wind speed.

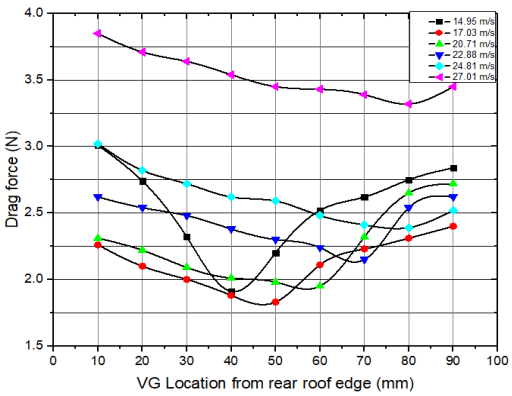

Fig. 6b. Drag force with VG position.

6.3. Effect of VG located in the flow separation point of the model on Drag Reduction rate

From the Fig. 6h it is clear that maximum drag reduction is attained at higher wind speed due to the effect of VG located at the flow separation point when compared with the base car model. The drag reduction rate stands at minimal percentage at lower

wind speed even though the VG is located at flow separation point

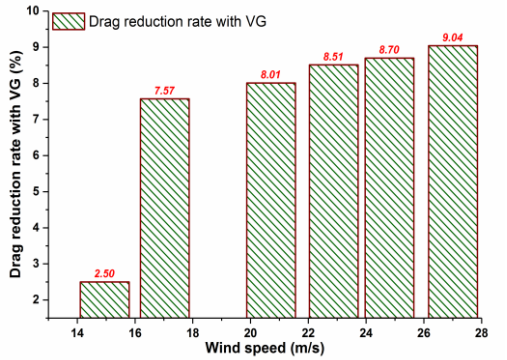

Fig. 6h Variation of drag reduction rate with VG location.

6.4. Effect of Drag on Power Consumption for Base Model and Model with VG

From the Fig. 6j it is understandable that the power consumption by the car model increases at all wind speeds to overcome the induced drag force. It is considerably reduced by the vortex generator when the wind blows at a speed greater than 20 m/s compared with the base model. It also indicates that the maximum power required when the wind has attained the maximum speed.

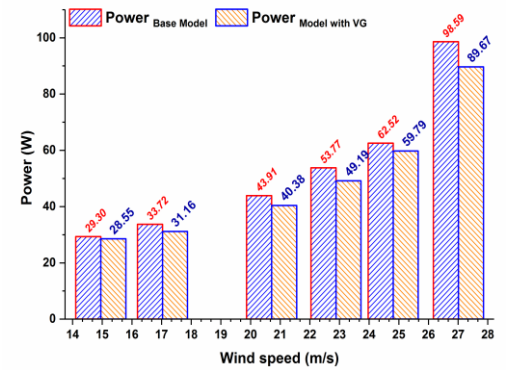

Fig. 6j. Variation of power consumption without and with VG on car model.

7. NUMERICAL ANALYSIS ON CAR MODEL

7.1 Pressure Distributions on Base Car Model and with VG Located 80 mm from Rear Edge at Wind Speed of 27.01 m/s

Fig. 7a shows the pressure distribution around the car model without and with VG positioned at 80 mm from the rear edge at the wind speed of 27.01 m/s. It shows that the flow separation is delayed around the VG location hence flow takes reattachment in the downstream and causes drag reduction. Harinaldi *et al* (2011). The drag coefficient was calculated numerically as 0.3187 with VG positioned at flow separation point and as 0.3414 without VG at higher wind speed of 27.01 m/s.

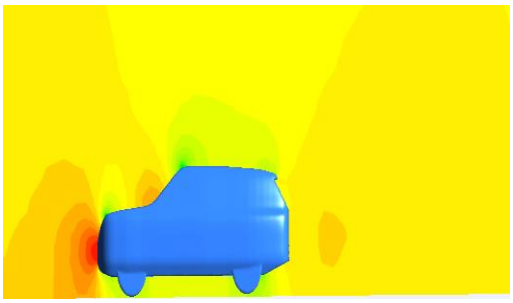

Without VG

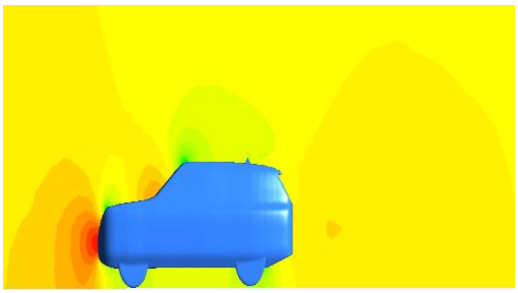

With VG

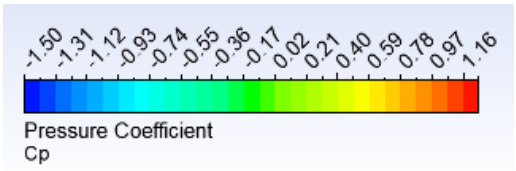

Fig. 7a. Variation of pressure coefficient around car model without and with VG.

7.2 Velocity Contour on Base Model and with VG Located at 80 mm from Rear Edge

Fig. 7b shows the velocity contour over the car profile without and with the effect of the VG. The numerical comparison results have shown that the wake region has decreased in the downstream due to the effect of the VG located at 80 mm from the rear edge; hence drag has reduced significantly at the wind speed of 27.01m/s.

7.3 Turbulence on Base Model and VG Located at 80 mm from Rear Edge

Fig.7c shows the turbulence induced when the fluid flow is over car model without and with the VG at the wind speed of 27.01 m/s. It confirms that the turbulence intensity has reduced significantly with the VG and eliminates flow separation in the downstream when compared with the base model. The fluid flow separated from the boundary layer causes the wake flow in downstream. The wake flow induces pressure drag which affects the performance of the vehicle.

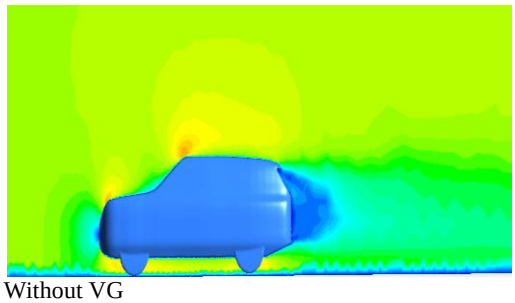

Without VG

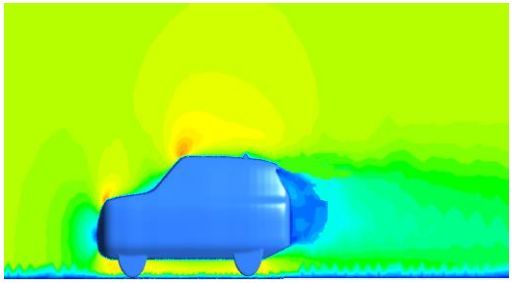

With VG

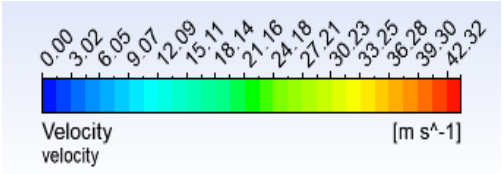

Fig. 7b. Velocity Contours around car model without and with VG.

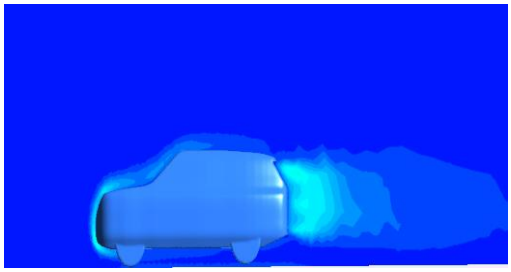

Without VG.

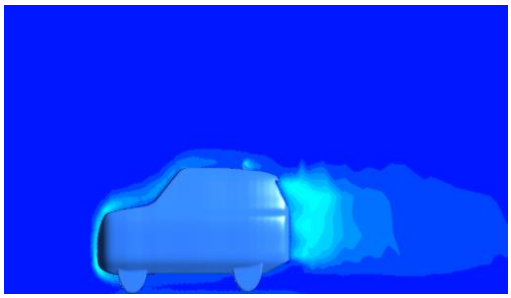

With VG

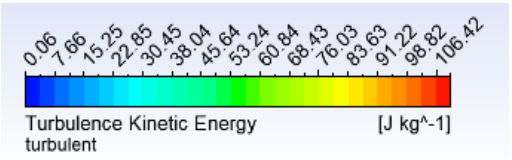

Fig. 7c. Turbulent intensity gradient around the car model without and with VG.

8. CONCLUSION

The pattern of the fluid flow was analyzed around the base car model with respect to wind speeds using wind tunnel. From the present work, it is found that the flow separation points changed with increase in wind speed and hence the position of the VG is optimized corresponding to wind speeds. The maximum drag reduction rate was calculated as 9.04 % and the power consumption was reduced by 8.92 W at maximum wind speed with the use of the optimized VG location when compared with base car model. The drag coefficient was determined as 0.3414 for the model without VG and got reduced to 0.3187 with VG located at flow separation point. The pressure coefficient, velocity contour and turbulent kinetic energy were studied numerically without and with the VG. The computational result showed good agreement with the experimental results by exhibiting minimum error deviation from the experimental findings.

ACKNOWLEDGEMENTS

The authors would like to express their sincere thanks to the Centre for Research, Anna University, Chennai, Tamilnadu, India and the Department of Aerospace Engineering for providing their technical support throughout this research.

REFERENCES

Agarwal, S., and P. Kumar (2016). Numerical Investigation of Flow Field and Effect of Varying Vortex Generator Location on Wing Performance. *American Journal of Fluid Dynamics* 26(1), 11-19.

Aider, J L., J. F. Beaudoin and J. E. Wesfreid (2010). Drag and lift reduction of a 3D bluff-body using active vortex generators. *Exp Fluids* 48, 771-789.

Al-Garni, A. M., L. P. Bernal and B. Khalighi (2004). Experimental investigation of the flow around a generic SUV. *SAE* 2004-01-0228.

Bansal, R and R. B. Sharma (2014). Drag Reduction of Passenger Car Using Add-On Devices. *Journal of Aerodynamics* 2014, 1-13.

Fukuda, H., K. Yanagimoto, H. China and K. Nakagawa (1995). Improvement of vehicle aerodynamics by wake control. *JSAE Review* 16, 151-155.

Gopal, P. and T. Senthilkumar (2012). Aerodynamic drag reduction in a passenger vehicle using vortex generator with varying yaw angles. *ARPN Journal of Engineering and Applied Sciences* 7(9), 1180-1186.

Grosche, F. R. and G. E. A. Meier (2011). Research at DLR Gottingen On bluff body aerodynamic, drag reduction by wake ventilation and active flow control. *Journal*

of Wind Engineering and Industrial Aerodynamics 89, 1201-1218.

Guo, L., Y. Zhang and W. J. Shen (2011). Simulation Analysis of Aerodynamics Characteristics of Different Two-Dimensional Automobile Shapes. *Journal of computers* 6(5), 999-1005.

Harinaldi, B., R. Tarakka and S. P. Simanunkalit (2011). Computational analysis of active flow control to reduce aerodynamics drag on a van model. *International journal of Mechanical & Mechatronics* 11(03), 24-30.

Hasan Ali, M., M. Mashud , A. Al Bari and M. Misbah-Ul Islam (2012). Aerodynamic Drag Reduction of a Car by Vortex Generation. *International Journal of Mechanical Engineering* 2(1), 12-21.

Hassan, S .M. R., T. Islam, M. Ali, and MQ. Islam (2014). Numerical Study on Aerodynamic Drag Reduction of Racing Cars. *Science Direct. Procedia Engineering* 90, 308 - 313.

Heinemann, T., M. Springer, H. Lienhart, S. Kniesburges and S. Becker (2014). Active Flow Control on a 1:4 Car Model. *Experiments in Fluids* 55(5), 1738

Howell, J., M. A. Passmore and S. Tuplin (2013). Aerodynamic Drag Reduction on a Simple Car-Like Shape with Rear Upper Body Taper. *SAE Int. J. Passeng. Cars - Mech. Syst.* 6(1), 52-60.

Hu, X. X., and T. T Wong (2011). A Numerical Study On Rear-spoiler Of Passenger Vehicle. *International Journal of Mechanical and Mechatronics Engineering* 5(9), 1800- 1805.

HU, X., R. Zhanga, J. Ye, X. Yan, and Z. Zhao (2011). Influence of Different Diffuser Angle on Sedan's Aerodynamic Characteristics. *Physics Procedia* 22, 239-245.

Jahanmiri, M. and M. Abbaspour (2011). Experimental investigation of drag reduction on Ahmed car model using a combination of active on flow control method. *IJE Transactions A: Basics* 24 (4), 403-410.

Khaled, M., H. El. Hage, F. Harambat, and H. Peerhossaini (2012). Some innovative concepts for car drag reduction: A parametric analysis of aerodynamic forces on a simplified body. *Journal of Wind Engineering and Industrial Aerodynamics* 107-108, 36-37.

Park, H., J. H Cho, J. Lee, D. H. Lee and K. H. Kim (2013). Experimental study of synthetic jets Array for Aerodynamic drag reduction of simplified car. *Journal of Mechanical science and Technology* 27(12), 3721-3731

Song, K .S., S. O. Kang, S. O. Jun, H. I. Park, J. D. Kee, K. H. Kim, And D. H. Lee (2012). *International Journal of Automotive Technology* 13(6), 905-914.

Wieser, D., H. Schmidt, S. Müller, C. Strangfeld, Christian Nayeri, and Christian Paschereit (2014). Experimental Comparison of the Aerodynamic Behavior of Fastback and Notchback DrivAer Models. *SAE Int. J. Passeng. Cars - Mech. Syst.* 7(2), 682-691.